Hue University Journal of Science: Natural Science
Vol. 131, No. 1D, 5–11, 2022

pISSN 1859-1388
eISSN 2615-9678

First-principles study on the structural and electronic properties of single-layer $MoSi_2N_4$

Cuong Q. Nguyen[1,2*], Le Thi Thu Phuong[1], Chuong V. Nguyen[3*]

[1] Department of Physics, University of Education, Hue University, 34 Le Loi St., Hue, Vietnam
[2] Institute of Research and Development, Duy Tan University, 3 Quang Trung St., Da Nang, Vietnam
[3] Department of Materials Science and Engineering, Le Quy Don Technical University, 236 Hoang Quoc Viet St., Hanoi, Vietnam

* Correspondence to Chuong V. Nguyen <chuong.vnguyen@lqdtu.edu.vn>

(*Received: 21 September 2021; Accepted: 19 January 2022*)

Abstract. Motivated by the successful exfoliation of a novel two-dimensional $MoSi_2N_4$ materials, in this work, we investigate the structural and electronic properties of a novel single-layer $MoSi_2N_4$ and the effect of strain engineering by using the first-principles calculations based on the density functional theory. The single-layer $MoSi_2N_4$ has a hexagonal structure with a space group of P6m1, which is dynamically stable. The material exhibits a semiconducting characteristic with an indirect band gap of 1.80/2.36 eV calculated by using the PBE/HSE functional. The conduction band minimum at the K point of the material originates from the Mo atom, while its valence band maximum at the Γ point is contributed by the hybridization between the Mo and N atoms. The electronic properties of the single-layer $MoSi_2N_4$ can be modulated with strain engineering, giving rise to a transition from a semiconductor to a metal and tending to a change in the band gap. Our results demonstrate that the single-layer $MoSi_2N_4$ is a promising candidate for electronic and optoelectronic applications.

Keywords: two-dimensional materials, strain engineering, first-principles calculations, single-layer $MoSi_2N_4$

1 Introduction

Recently, two-dimensional (2D) materials have received tremendous interest owing to their extraordinary physical properties and potential applications [1-3]. Graphene [4] has emerged as one of the most promising 2D materials owing to its superior properties, including excellent carrier mobility [5] and superior thermal conductivity [6], making it suitable for high-performance electronic devices [7, 8]. However, the absence of a sizable band gap in graphene restricts its applications in high-performance logic circuit applications. To overcome this limitation, researchers have been seeking other novel 2D materials, including transition metal dichalcogenides (TDMs) [9], phosphorene [10, 11], and *h*-BN [12, 13]. Unlike graphene, these 2D materials are semiconductors with a moderate band gap of about 2 eV, which is appropriate for designing electronic nanodevices. However, the carrier mobility in most 2D TMDs is not as high as that of graphene [14], limiting their applications in electronics. In contrast to 2D TMDs, phosphorene exhibits high carrier mobility [15]. The instability of phosphorene under ambient conditions [16] makes it unsuitable for optoelectronic applications. The search for novel 2D materials with desired properties is still a challenge.

More recently, a new type of 2D material, single-layer $MoSi_2N_4$, has been successfully synthesized with the chemical vapour deposition

(CVD) method [17]. Single-layer $MoSi_2N_4$ is environmentally stable at ambient temperature and exhibits an indirect band gap and high intrinsic thermal conductivity [18]. The electronic and optical properties of bilayer $MoSi_2N_4$ are very sensitive to strain engineering and electric field [19]. Various strategies have been developed to modulate the properties of single-layer $MoSi_2N_4$, including doping [20], strain engineering [21] and constructing heterostructures [19, 22]. For instance, by means of first-principles calculations, Cui et al. [20] demonstrated that the electronic properties of single-layer $MoSi_2N_4$ can be modulated with molecular doping. Guo et al. predicted that the transport coefficients of single-layer $MoSi_2N_4$ are enhanced under biaxial strain. All aforementioned findings suggest that single-layer $MoSi_2N_4$ plays a crucial role in designing future electronic and optoelectronic devices.

Therefore, in this work, using first-principles calculations based on density functional theory, we investigate the electronic properties of single-layer $MoSi_2N_4$ and the effect of strain engineering. Our findings could provide useful insight into the design of high-performance nanodevices based on 2D single-layer $MoSi_2N_4$.

2 Computational methods

In this work, we present our results of the geometric optimization and electronic properties of single-layer $MoSi_2N_4$, obtained from the first-principles calculations based on density functional theory (DFT), which is implemented in the Vienna ab initio simulation package (VASP) [23, 24]. The generalized gradient approximation (GGA) with Perdew-Burke-Ernzerhof (PBE) functional [25] was employed to describe the electronic exchange and correlation. The projector-augmented wave (PAW) approach [48] was chosen to treat the core and valence electrons. The underestimation of the traditional PBE method on the band gap of 2D materials led us to use the Heyd-Scuseria-Ernzerhof (HSE06) hybrid functional [26] to obtain a more accurate value of band gap. The DFT-D2 method was also adopted for describing the existing van der Waals interactions in layered materials. The cut-off energy for the plane-wave expansion was set to 410 eV with a 9 × 9 × 1 k-point mesh. To avoid interactions between periodical slabs, we set a large vacuum thickness to 20 Å along the z direction. The convergence of energy and force are set to 1×10^{-6} eV and 1×10^{-3} eV/Å.

3 Results and discussions

The atomic structure of the single-layer $MoSi_2N_4$ after geometric optimization is depicted in Fig. 1. One can find that the material has a hexagonal structure with a space group of P6m1. The material shows a layered atomic structure. The Mo-N_2 layer is sandwiched between two Si-N layers. The lattice parameter of the material after geometric optimization is 2.9 Å, which is in good agreement with the previous reports [17, 27].

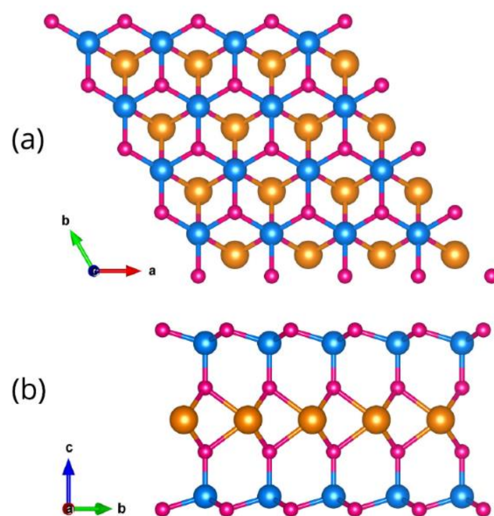

Fig. 1. (a) Top view and (b) side view of the atomic structure of single-layer $MoSi_2N_4$ after geometric optimization. Purple, blue and yellow balls represent the nitrogen, silicon and molybdenum atoms

pISSN 1859-1388
eISSN 2615-9678

We now move to check the dynamical stability of the $MoSi_2N_4$ single layer by calculating its phonon dispersions curves, as depicted in Fig. 2. We can find that the phonon dispersions of such a material do not include any negative frequencies, suggesting that the single-layer $MoSi_2N_4$ is dynamically stable at the ground state. The single-layer $MoSi_2N_4$ consists of all its seven atoms in each unit cell, thus, resulting in the presence of 21 branches: 3 acoustical and 18 optical branches. The three acoustical phonon dispersion branches at the Γ point correspond to an out-of-plane mode (ZA), an in-plane transverse mode (TA), and an in-plane longitudinal (LA). Furthermore, to check the thermal stability of such a monolayer, we calculated the variations of the total energy of the single-layer $MoSi_2N_4$ as a function of time step by performing AIMD simulations, as depicted in Fig. 3. We see that the single-layer $MoSi_2N_4$ still maintains its crystal structure after heating for 4 ps, suggesting that the material exhibits good thermal stability at ambient temperature.

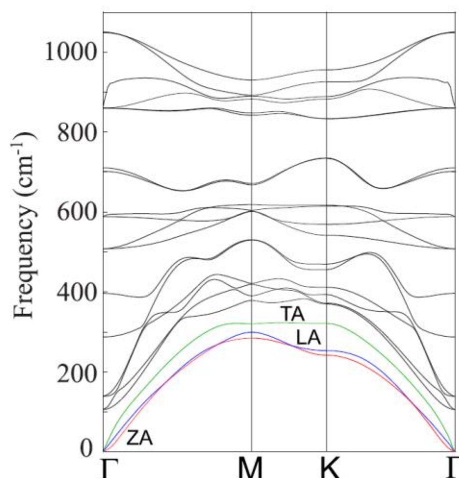

Fig. 2. Phonon dispersion curves of single-layer $MoSi_2N_4$ at the ground state

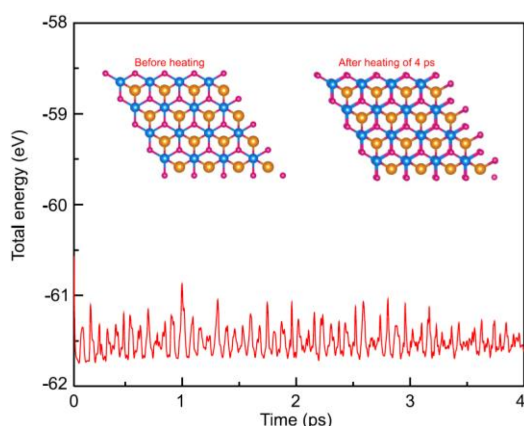

Fig. 3. Evolution of total energy of single-layer $MoSi_2N_4$ in AIMD simulation. The insets represent the snapshot structures of single-layer $MoSi_2N_4$ before and after heating for 4 ps at 300 K

The band structure of the single-layer $MoSi_2N_4$ obtained from the PBE method is illustrated in Fig. 4. We can observe that the material exhibits a semiconducting characteristic with an indirect band gap. The valence band maximum (VBM) of the single-layer $MoSi_2N_4$ originates from the Γ point, while its conduction band minimum (CBM) is located at the K point, as depicted in Fig. 4a. The band gap of the single-layer $MoSi_2N_4$ is 1.8 eV calculated with the PBE method. Such a band gap is in good agreement with the experimental measurement (1.94 eV) [17] and other theoretical reports [22, 28]. Furthermore, to obtain a more accurate band gap, we plotted the band structure of the single-layer $MoSi_2N_4$ by using the HSE06 functional for comparison (Fig. 4b). The band gap of the single-layer $MoSi_2N_4$ given by the HSE06 functional is 2.38 eV, which is still larger than that of experimental measurement. In addition, both the PBE and HSE06 functionals predict a similar trend of the band structure of single-layer $MoSi_2N_4$. The difference in the band gap of single-layer $MoSi_2N_4$ between PBE and HSE06 functionals is due to the upshift/downshift of the CBM/VBM of the single-layer $MoSi_2N_4$. All aforementioned findings suggest that the PBE functional can be used to investigate the structural and electronic properties of single-layer $MoSi_2N_4$.

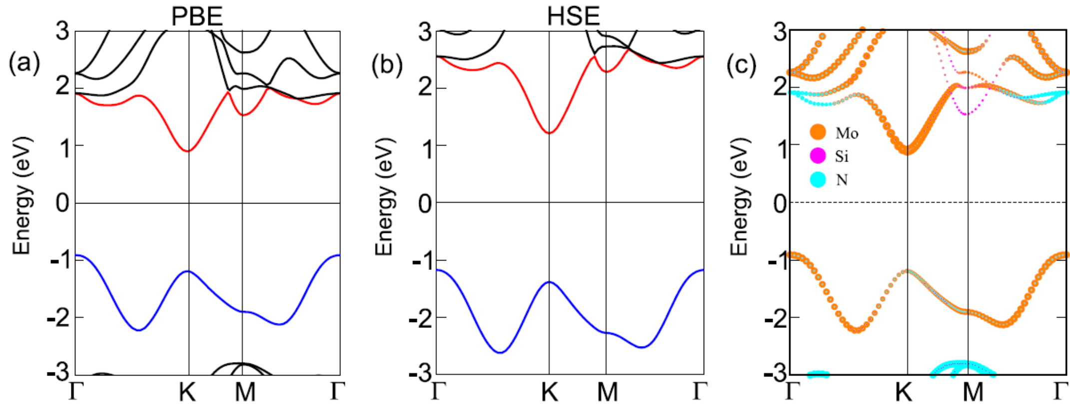

Fig. 4. Band structures given of single-layer $MoSi_2N_4$ by (a) PBE and (b) HSE functional. The red and blue curves represent the CBM and VBM. (c) Weighted band structure of single-layer $MoSi_2N_4$. The yellow, purple and cyan balls stand for the contributions of Mo, Si and N atoms, respectively. The Fermi level is set to zero.

To have a better understanding of the contributions of all atoms in the single-layer $MoSi_2N_4$, we further calculated its weighted band structure, as illustrated in Fig. 4c. Yellow, purple and cyan curves in the weighted band structure of the material represent the contribution of molybdenum, silicon, and nitrogen atoms. One can find that the CBM at the K point of the single-layer $MoSi_2N_4$ originates from the Mo atom, while the VBM at the Γ point is mainly contributed by the hybridization between Mo and N atoms.

Interestingly, strain engineering is known as one of the effective strategies to modulate the electronic properties of 2D materials, including graphene [29, 30], TMDs [31, 32], and phosphorene [33, 34]. Therefore, it is interesting to explore whether the electronic properties of the single-layer $MoSi_2N_4$ can be controlled by strain engineering. The strain is applied along the *xy* direction, as depicted in the inset of Fig. 5. The strain ratio is defined as $\varepsilon_b = (l_0 - l)/l_0$, where l and l_0 represent the equilibrium and strained lattice parameters of single-layer $MoSi_2N_4$. In addition, to evaluate the stability of the single-layer $MoSi_2N_4$ under strain, we further calculate the strain energy as $E_s = E_{strain} - E_{Eq}$, where E_{strain} and E_{Eq} are the total energy of the single-layer $MoSi_2N_4$ under strain and at the equilibrium state. We found that the calculated strain energy of the material under the strain of 12% is –6.53 eV. This finding indicates that all the strains considered are fully reversible and are within the elastic limit. Therefore, the lattice structure could maintain stability under the considered strains.

The effect of strain on the band gap of the single-layer $MoSi_2N_4$ is depicted in Fig. 5. We can see that the band gap of the material decreases with increasing tensile strain. For instance, the band gap decreases from 1.8 eV when ε_b = 0% to 1.04 eV when ε_b = 6% and to 0.62 eV when ε_b = 12%. Our calculations demonstrate that under the tensile strain of 18%, the band gap of the single-layer $MoSi_2N_4$ decreases to nearly zero, indicating

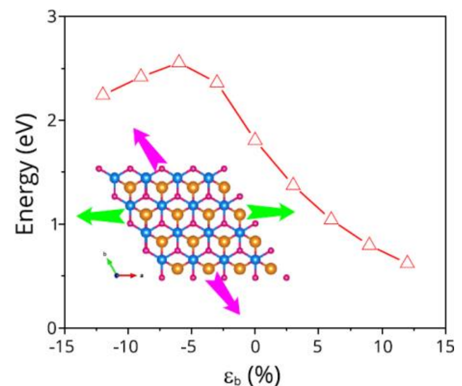

Fig. 5. Evolution of the band gap as a function of strain engineering. The inset represents the schematic model of applying strain

pISSN 1859-1388
eISSN 2615-9678

a transition from semiconductor to metal. On the other hand, with decreasing the small compressive strain, ranging from 0 to –6%, the band gap of single-layer $MoSi_2N_4$ increases accordingly. The band gap of the single-layer $MoSi_2N_4$ reaches its maximum value of 2.55 eV under the compressive strain of –6%. With a continuing decrease of the compressive strain from –6% to –12%, the band gap of the material decreases from 2.55 to 2.24 eV.

To have a better understanding of the controllable band gap of the single-layer $MoSi_2N_4$ under strain, we further calculated its band structures under different compressive and tensile strains (Fig. 6). Under the compressive strain of –3%, as depicted in Fig. 6d, the material keeps a semiconducting characteristic with an indirect band gap, in which the CBM is at K point and the VBM is at the Γ point. Under the compressive strain of –6%, the VBM shifted from the K to M point, whereas the VBM shifted from the Γ to K point, as shown in Fig. 6c. In this case, the single-layer $MoSi_2N_4$ behaves as an indirect semiconductor. With a continuing decrease of the compressive strain to –9 and –12%, both the VBM at the K point and CBM at the M point of the

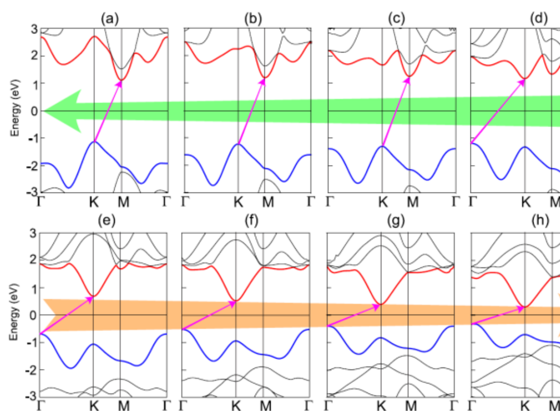

Fig. 6. Band structures of single-layer $MoSi_2N_4$ under different strain engineering of (a) $\varepsilon_b = -12\%$, (b) $\varepsilon_b = -9\%$, (c) $\varepsilon_b = -6\%$, (d) $\varepsilon_b = -3\%$, (e) $\varepsilon_b = +3\%$, (f) $\varepsilon_b = +6\%$, (g) $\varepsilon_b = +9\%$, and (h) $\varepsilon_b = +12\%$. The Fermi level is set to zero. Red and blue curves represent the CBM and VBM of single-layer $MoSi_2N_4$

single-layer $MoSi_2N_4$ tend to shift toward the Fermi level, resulting in the decrease in its band gap. On the other hand, under the tensile strain, both the VBM and CBM of the material move toward the Fermi level, reducing the band gap. Under the tensile strain, the VBM of the single-layer $MoSi_2N_4$ is maintained at the Γ point, and the CBM is maintained at the K point. Thus, an indirect band gap semiconductor is also maintained in the material under the tensile strain. Because the band gap of the material exhibits a linear change under tensile strain, it may lead to a transition from semiconductor to metal at the critical tensile strain. Our findings suggest that at the tensile strain of +18%, both the VBM and CBM of the single-layer $MoSi_2N_4$ shifts toward the Fermi level and crosses the Fermi level, resulting in a transition from semiconductor to metal. All aforementioned findings demonstrate that strain engineering can be used to modulate the electronic properties of the single-layer $MoSi_2N_4$ with a transition from semiconductor to metal. Our findings indicate that single-layer $MoSi_2N_4$ is a promising candidate for electronic and optoelectronic applications.

4 Conclusion

In summary, we performed first-principles calculations to study the structural and electronic properties of a novel single-layer 2D $MoSi_2N_4$. The effect of strain engineering on the band gap and electronic properties of the single-layer 2D $MoSi_2N_4$ is also considered. Our results show that the single-layer $MoSi_2N_4$ has a hexagonal structure with a space group of P6m1. At the ground state, the material is dynamically stable and is a semiconductor with an indirect band gap of 1.8/2.36 eV calculated by using the PBE/HSE06 functionals. The band gap of the material can be modulated with strain engineering. The tensile strain leads to a decrease in the band gap, while under the compressive strain, the band gap

increases first, then decreases with increasing the compressive strain. The band gap of the single-layer $MoSi_2N_4$ reaches its maximum value at the compressive strain of –6%. Furthermore, under the tensile strain, the transition from semiconductor to metal can be achieved. Our results demonstrate that the single-layer $MoSi_2N_4$ is a promising candidate for electronic and optoelectronic applications.

References

1. Fiori G, Bonaccorso F, Iannaccone G, Palacios T, Neumaier D, Seabaugh A, et al. Electronics based on two-dimensional materials. Nature Nanotechnology. 2014;9(10):768-779.
2. Miró P, Audiffred M, Heine T. An atlas of two-dimensional materials. Chemical Society Reviews. 2014;43(18):6537-6554.
3. Butler SZ, Hollen SM, Cao L, Cui Y, Gupta JA, Gutiérrez HR, et al. Progress, challenges, and opportunities in two-dimensional materials beyond graphene. ACS Nano. 2013;7(4):2898-2926.
4. Novoselov KS, Geim AK, Morozov SV, Jiang D, Zhang Y, Dubonos SV, et al. Electric field effect in atomically thin carbon films. Science. 2004;306(5696):666-669.
5. Novoselov KS, Geim AK, Morozov SV, Jiang D, Katsnelson MI, Grigorieva I, et al. Two-dimensional gas of massless dirac fermions in graphene. Nature. 2005;438(7065):197-200.
6. Balandin AA, Ghosh S, Bao W, Calizo I, Teweldebrhan D, Miao F, et al. Superior thermal conductivity of single-layer graphene. Nano Letters. 2008;8(3):902-907.
7. Zhan B, Li C, Yang J, Jenkins G, Huang W, Dong X. Graphene field-effect transistor and its application for electronic sensing. Small. 2014;10(20):4042-4065.
8. Xia F, Mueller T, Lin YM, Valdes-Garcia A, Avouris P. Ultrafast graphene photodetector. Nature Nanotechnology. 2009;4(12):839-843.
9. Manzeli S, Ovchinnikov D, Pasquier D, Yazyev OV, Kis A. 2D transition metal dichalcogenides. Nature Reviews Materials. 2017;2(8):1-15.
10. Carvalho A, Wang M, Zhu X, Rodin AS, Su H, Neto AHC. Phosphorene: From theory to applications. Nature Reviews Materials. 2016;1(11):1-16.
11. Kou L, Chen C, Smith SC. Phosphorene: Fabrication, properties, and applications. Journal of Physical Chemistry Letters. 2015;6(14):2794-2805.
12. Cassabois G, Valvin P, Gil B. Hexagonal boron nitride is an indirect bandgap semiconductor. Nature Photonics. 2016;10(4):262-266.
13. Zhang K, Feng Y, Wang F, Yang Z, Wang J. Two dimensional hexagonal boron nitride (2D-hBN): Synthesis, properties and applications. Journal of Materials Chemistry C. 2017;5(46):11992-12022.
14. Zhou H, Wang C, Shaw JC, Cheng R, Chen Y, Huang X, Liu Y, Weiss NO, Lin Z, Huang Y. Large area growth and electrical properties of p-type WSe_2 atomic layers. Nano Letters. 2015;15(1):709-713.
15. Liu H, Neal AT, Zhu Z, Luo Z, Xu X, Tománek D, et al. Phosphorene: An unexplored 2D semiconductor with a high hole mobility. ACS Nano. 2014;8(4):4033-4041.
16. Jain R, Singh Y, Cho S-Y, Sasikala SP, Koo SH, Narayan R, et al. Ambient stabilization of few layer phosphorene via noncovalent functionalization with surfactants: Systematic 2D NMR characterization in aqueous dispersion. Chemistry of Materials. 2019;31(8):2786-2794.
17. Hong YL, Liu Z, Wang L, Zhou T, Ma W, Xu C, et al. Chemical vapor deposition of layered two-dimensional $MoSi_2N_4$ materials. Science. 2020;369(6504):670-674.
18. Yu J, Zhou J, Wan X, Li Q. High intrinsic lattice thermal conductivity in monolayer $MoSi_2N_4$. New Journal of Physics. 2021;23(3):033005.
19. Wu Q, Cao L, Ang YS, Ang LK. Semiconductor-to-metal transition in bilayer $MoSi_2N_4$ and WSi_2N_4 with strain and electric field. Applied Physics Letters. 2021;118(11):113102.
20. Cui Z, Luo Y, Yu J, Xu Y. Tuning the electronic properties of $MoSi_2N_4$ by molecular doping: A first principles investigation. Physica E: Low-dimensional Systems and Nanostructures. 2021;134(114873.
21. Guo XS, Guo SD. Tuning transport coefficients of monolayer $MoSi_2N_4$ with biaxial strain. Chinese Physics B. 2021;30(6):067102.

pISSN 1859-1388
eISSN 2615-9678

22. Cao L, Zhou G, Wang Q, Ang L, Ang YS. Two-dimensional van der waals electrical contact to monolayer $MoSi_2N_4$. Applied Physics Letters. 2021;118(1):013106.

23. Kresse G, Hafner J. Ab initio molecular dynamics for liquid metals. Physical Review B. 1993;47(1):558.

24. Kresse G, Furthmüller J. Efficient iterative schemes for ab initio total-energy calculations using a plane-wave basis set. Physical Review B. 1996;54(16):11169.

25. Perdew JP, Burke K, Ernzerhof M. Generalized gradient approximation made simple. Physical Review Letters. 1996;77(18):3865.

26. Heyd J, Scuseria GE, Ernzerhof M. Hybrid functionals based on a screened coulomb potential. Journal of Chemical Physics. 2003;118(18):8207-8215.

27. Pham KD, Nguyen CQ, Nguyen C, Cuong PV, Hieu NV. Two-dimensional van der waals graphene/transition metal nitride heterostructures as promising high-performance nanodevices. New Journal of Chemistry. 2021;45(12):5509-5516.

28. Bafekry A, Faraji M, Hoat D, Shahrokhi M, Fadlallah M, Shojaei F, et al. $MoSi_2N_4$ single-layer: A novel two-dimensional material with outstanding mechanical, thermal, electronic and optical properties. Journal of Physics D: Applied Physics. 2021;54(15):155303.

29. Choi SM, Jhi SH, Son YW. Effects of strain on electronic properties of graphene. Physical Review B. 2010;81(8):081407.

30. Si C, Sun Z, Liu F. Strain engineering of graphene: A review. Nanoscale. 2016;8(6):3207-3217.

31. Shen T, Penumatcha AV, Appenzeller J. Strain engineering for transition metal dichalcogenides based field effect transistors. ACS Nano. 2016;10(4):4712-4718.

32. Kansara S, Gupta SK, Sonvane Y. Effect of strain engineering on 2D dichalcogenides transition metal: A DFT study. Computational Materials Science. 2018;141(235-242.

33. Sa B, Li YL, Qi J, Ahuja R, Sun Z. Strain engineering for phosphorene: The potential application as a photocatalyst. Journal of Physical Chemistry C. 2014;118(46):26560-26568.

34. Phuc HV, Hieu NN, Ilyasov VV, Phuong L, Nguyen CV. First principles study of the electronic properties and band gap modulation of two-dimensional phosphorene monolayer: Effect of strain engineering. Superlattices and Microstructures. 2018;118(289-297.